

## Precision Mass Measurements beyond $^{132}\text{Sn}$ : Anomalous Behavior of Odd-Even Staggering of Binding Energies

J. Hakala,\* J. Dobaczewski, D. Gorelov, T. Eronen,† A. Jokinen, A. Kankainen, V. S. Kolhinen, M. Kortelainen, I. D. Moore, H. Penttilä, S. Rinta-Antila, J. Rissanen, A. Saastamoinen, V. Sonnenschein, and J. Äystö‡

*Department of Physics, P.O. Box 35 (YFL), FI-40014 University of Jyväskylä, Finland*

(Received 5 March 2012; published 16 July 2012)

Atomic masses of the neutron-rich isotopes  $^{121-128}\text{Cd}$ ,  $^{129,131}\text{In}$ ,  $^{130-135}\text{Sn}$ ,  $^{131-136}\text{Sb}$ , and  $^{132-140}\text{Te}$  have been measured with high precision (10 ppb) using the Penning-trap mass spectrometer JYFLTRAP. Among these, the masses of four  $r$ -process nuclei  $^{135}\text{Sn}$ ,  $^{136}\text{Sb}$ , and  $^{139,140}\text{Te}$  were measured for the first time. An empirical neutron pairing gap expressed as the odd-even staggering of isotopic masses shows a strong quenching across  $N = 82$  for Sn, with a  $Z$  dependence that is unexplainable by the current theoretical models.

DOI: [10.1103/PhysRevLett.109.032501](https://doi.org/10.1103/PhysRevLett.109.032501)

PACS numbers: 21.10.Dr, 21.60.-n, 27.60.+j

The doubly magic  $^{132}\text{Sn}$  nucleus has been probed intensively by nuclear spectroscopy over the last two decades. It has been found to exhibit features of exceptional purity for its single particle structure [1,2]. This provides an ideal starting point for exploring the detailed evolution of nuclear structure of more neutron-rich nuclei beyond the  $N = 82$  closed shell in the vicinity of Sn. Only a few experimental and theoretical attempts along these lines have been performed recently. No experimental data exist for excited states or masses for nuclides below Sn with  $N > 82$ . The experimental situation is slightly better for the  $Z > 50$  isotopes of Sb and Te because of their easier access.

Recent data on the  $B(E2)$  transition strengths for  $^{132}\text{Te}$ ,  $^{134}\text{Te}$ , and  $^{136}\text{Te}$  isotopes [3], and their interpretation using a quadrupole-plus-pairing Hamiltonian and the quasiparticle random phase approximation [4] suggested the need for reduced neutron pairing to explain the observed anomalous asymmetry in the  $B(E2)$  values across the  $N = 82$  neutron shell. This behavior was not observed in standard shell model calculations [3]. Another shell model calculation of the binding energies of heavy Sn isotopes with  $A > 133$  [5] suggested the importance of pairing correlations and the strength of the pairing interaction in general for weakly bound nuclei. Therefore, it would be necessary to probe the evolution of odd-even staggering of masses [6] around the  $N = 82$  neutron shell to learn about the magnitude of pairing and its variation as a function of  $Z$  and  $N$  beyond  $^{132}\text{Sn}$ .

The high precision of present-day ion-trap mass spectrometry combined with the high sensitivity [7] can provide the needed information on mass differences such as one- and two-nucleon separation energies, shell gaps, and empirical pairing energies. For example, the masses of neutron-rich Sn and Xe isotopes were recently measured up to  $^{134}\text{Sn}$  and  $^{146}\text{Xe}$  with the Penning-trap mass spectrometer ISOLTRAP at the CERN ISOLDE facility [8,9]. In this Letter we wish to present new data of high-precision mass measurements of neutron-rich Cd, In, Sn, Sb, and Te

isotopes across the  $N = 82$  neutron shell by using the JYFLTRAP Penning trap. These nuclides are also of interest for nuclear astrophysics models of element synthesis, in particular, to explain the large  $r$ -process abundance peak at  $A = 130$  [10] (see Fig. 1). In more general context, a vast body of nuclear data on neutron-rich isotopes is needed for  $r$ -process nucleosynthesis predictions. Such data include masses, single particle spectra, pairing characteristics, as well as decay properties and reaction rates. In all of these the binding energies or masses of ground, isomeric, and excited states play key roles [10].

The measurements were performed using the JYFLTRAP Penning-trap mass spectrometer [11] which is connected to the Ion Guide Isotope Separator On-Line (IGISOL) mass separator [12]. The ions of interest were produced in proton-induced fission reactions by bombarding a natural uranium target with a proton beam of 25 MeV energy. A thorium target was used in the case of  $^{129}\text{In}$  and isotopes of Sb.

Fission products stopped in a helium-filled gas cell at a pressure of about 200 mbar as singly charged ions were transported out of the gas cell, accelerated to 30 keV energy, and mass separated. A gas-filled radio frequency

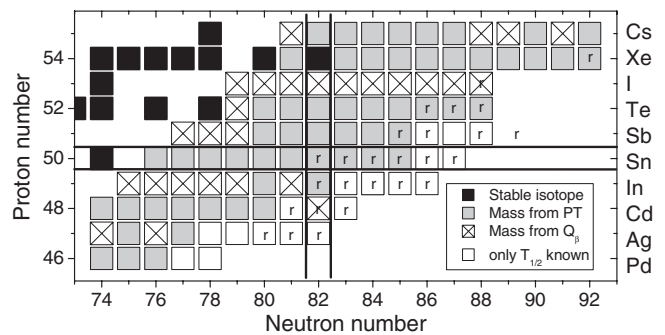


FIG. 1. Neutron-rich isotopes with  $T_z \geq 13$  whose masses have been determined by Penning trap (PT) or  $Q_\beta$  measurements. Letter  $r$  denotes  $r$ -process nuclei according to Ref. [10].

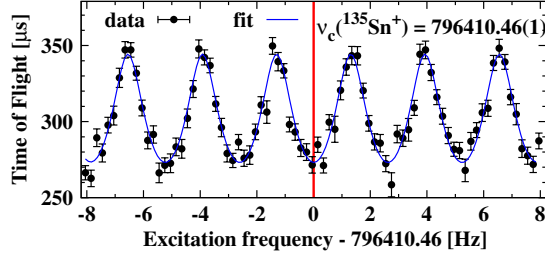


FIG. 2 (color online). A time-of-flight resonance from the JYFLTRAP setup for  $^{135}\text{Sn}^+$ . A two-fringe Ramsey pattern of 25-350-25 ms (*on-off-on*) was used in this case.

quadrupole cooler and buncher prepared the ions for the Penning-trap setup.

In a Penning trap an ion has three different eigenmotions: axial motion ( $\nu_z$ ) and two radial motions, magnetron

( $\nu_-$ ) and modified cyclotron ( $\nu_+$ ) motion. The frequencies of the radial motions sum in first order to the cyclotron frequency  $\nu_c = \frac{1}{2\pi} \frac{q}{m} B$ . Here  $q$  and  $m$  are the charge and mass of the ion, and  $B$  is the magnetic field.

JYFLTRAP consists of two cylindrical Penning traps, the purification and precision trap, which are located inside a 7-T superconducting magnet. Both traps were used to purify the samples, first with the sideband cooling technique [13] for isobaric separation and then, if prompted by the presence of isomers or other contaminants, with the Ramsey cleaning technique [14]. After a cleaned sample was trapped in the precision trap, the time-of-flight ion-cyclotron resonance technique [15] was applied in order to determine the resonance frequency. The Ramsey method of separated oscillatory fields [16], which makes the sidebands more pronounced and narrower, was used in the

TABLE I. Cyclotron frequency ratios  $\bar{\nu}$  and ground state mass excess values in keV based on this work. Masses of reference Xe isotopes in column 1 for given  $A$  are from Refs. [20–22]. Results from other direct mass measurements are from ISOLTRAP [8,23,24] or an experimental storage ring (ESR) at the fragment separator (FRS) [25]. Otherwise, the value from Atomic Mass Evaluation 2003 (AME2003) [20] is given.

Xe A	Nuclide	$\bar{\nu} = \frac{\nu_{c,\text{ref}}}{\nu_{c,\text{meas}}}$	JYFLTRAP keV	Literature keV	Ref.
130	$^{121}\text{Cd}^b$	0.930 790 292(23)	−81 074.2(28)	−81 060(80)	[20]
	$^{122}\text{Cd}$	0.938 492 175(22)	−80 610.8(27)	−80 616.6(44)	[24]
	$^{123}\text{Cd}^b$	0.946 216 645(22)	−77 414.4(26)	−77 367(93)	[24]
	$^{124}\text{Cd}$	0.953 920 584(26)	−76 702(4)	−76 697(10)	[24]
	$^{125}\text{Cd}^b$	0.961 646 357(24)	−73 348.1(29)	−73 360(70)	[20]
	$^{126}\text{Cd}$	0.969 353 430(25)	−72 257(3)	−72 256.5(42)	[24]
	$^{127}\text{Cd}$	0.977 082 59(11)	−68 493(13)	−68 520(70)	[20]
	$^{128}\text{Cd}$	0.984 791 049(83)	−67 234(10)	−67 250(17)	[24]
	$^{129}\text{In}$	0.992 442 788(22)	−72 838.0(26)	−72 940(40)	[20]
	$^{131}\text{In}$	1.007 878 672(22)	−68 025.0(26)	−68 137(28)	[20]
	$^{130}\text{Sn}$	1.000 080 552(28)	−80 133(4)	−80 134(16)	[23]
132	$^{131}\text{Sn}$	0.992 516 774(26)	−77 262(20) <sup>a</sup>	−77 264(10)	[8]
	$^{132}\text{Sn}$	1.000 103 654(26)	−76 543(4)	−76 547(7)	[8]
134	$^{133}\text{Sn}$	0.992 670 308(18)	−70 874.4(24)	−70 847(23)	[8]
	$^{134}\text{Sn}$	1.000 173 910(25)	−66 432(4)	−66 320(150)	[8]
130	$^{135}\text{Sn}$	1.038 731 983(25)	−60 632(3)		
	$^{131}\text{Sb}$	1.007 763 324(18)	−81 982.5(21)	−81 988(21)	[20]
	$^{132}\text{Sb}^b$	1.015 480 774(22)	−79 635.6(27)	−79 674(14)	[20]
	$^{133}\text{Sb}$	1.023 184 733(31)	−78 921(4)	−78 943(25)	[20]
	$^{134}\text{Sb}^b$	1.030 923 280(17)	−74 021.1(21)	−74 170(40)	[20]
	$^{135}\text{Sb}$	1.038 657 131(24)	−69 689.6(29)	−69 710(100)	[20]
	$^{136}\text{Sb}$	1.046 397 992(52)	−64 510(7)		
	$^{132}\text{Te}$	1.015 434 872(33)	−85 190(4)	−85 182(7)	[20]
	$^{133}\text{Te}^b$	1.023 151 534(18)	−82 938.2(22)	−82 945(24)	[20]
	$^{134}\text{Te}$	1.030 852 922(27)	−82 535(4)	−82 559(11)	[20]
	$^{135}\text{Te}$	1.038 590 701(22)	−77 727.9(26)	−77 725(123)	[20]
	$^{136}\text{Te}$	1.046 316 045(24)	−74 425.7(29)	−74 430(50)	[20]
	$^{137}\text{Te}$	1.054 056 424(21)	−69 304.2(25)	−69 290(120)	[25]
	$^{138}\text{Te}$	1.061 784 295(36)	−65 696(5)	−65 755(122)	[25]
	$^{139}\text{Te}$	1.069 527 729(29)	−60 205(4)		
	$^{140}\text{Te}$	1.077 257 59(23)	−56 357(27)		

<sup>a</sup>Corrected for 65.1 keV isomer; see Ref. [20].

<sup>b</sup>Isomer separated.

majority of measurements. The experimental setup and the measurement technique are described in more detail in Ref. [17].

A sample resonance is shown in Fig. 2. When the cyclotron frequencies of an unknown species ( $m_{\text{meas}}$ ) and a well-known reference ion ( $m_{\text{ref}}$ ) are known, and both are singly charged ions, the atomic mass can be determined as follows:

$$m_{\text{meas}} = \frac{\nu_{c,\text{ref}}}{\nu_{c,\text{meas}}} (m_{\text{ref}} - m_e) + m_e, \quad (1)$$

where  $m_e$  is the mass of the electron. The data analysis procedure was almost identical compared to Ref. [18]. In this work, the systematic uncertainties due to the magnetic field fluctuations were minimised by applying so-called interleaved frequency scanning, described in Ref. [19].

The results are given in Table I. Excitation times between 100 and 800 ms were used depending on the half-life of the isotope. In the case of Ramsey excitations, excitation patterns with two 25 ms pulses separated by a waiting time were used. Table I lists only the masses of the ground states which are relevant for the further discussion of the results. A paper containing the isomeric data will be submitted separately. The new data agree with the earlier ion-trap measurements and present significant improvement in accuracy for all Sn, Sb, and Te isotopes beyond  $N = 82$ .

The high precision of Penning-trap mass measurements enables for the first time a critical evaluation of odd-even staggering of binding energies and related empirical pairing gaps across the  $N = 82$  shell gap. The most simple example is the three-point odd-even-mass-staggering formula [6]

$$\Delta^{(3)}(N) = (-1)^N [E(N+1) - 2E(N) + E(N-1)]/2, \quad (2)$$

where  $N$  is the number of nucleons (neutrons or protons) and  $E$  the binding energy. The  $\Delta^{(3)}$  staggering mostly depends on the intensity of pairing correlations in nuclei, but, as we discuss below, it is also affected by the polarization effects.

Figure 3 shows the experimental neutron  $\Delta^{(3)}$  staggering for Sn, Te, and Xe isotopes crossing the  $N = 82$  shell closure. The difference between the values at  $N = 81$  and  $83$  shows a large asymmetry for Sn but a much smaller one for Te and Xe. This indicates a considerably stronger quenching in the pairing gap for Sn than for Te and Xe, suggesting the importance of core polarization effects. A similar asymmetry observed for  $B(E2)$  values of n-rich Te isotopes was also traced to reduced neutron pairing above the  $N = 82$  shell closure [4].

In order to probe this question theoretically, we performed self-consistent calculations of varying complexity, by using the Sly4 [26] energy density functional and contact pairing force. To make a meaningful comparison, in each variant of the calculation, the pairing strength (equal for

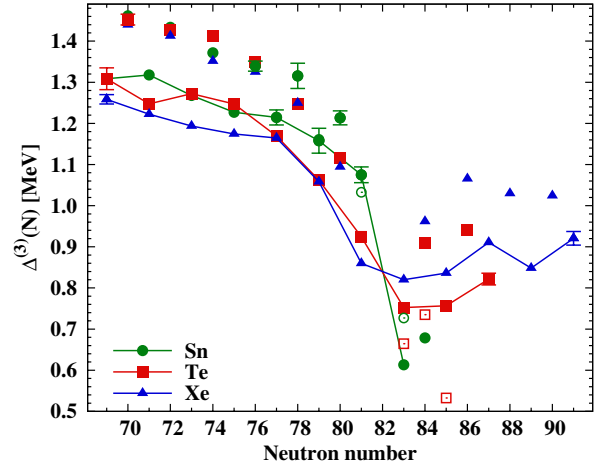


FIG. 3 (color online). Experimental odd-even mass staggering for Sn, Te, and Xe isotope chains. For clarity, odd- $N$  points have been connected with lines and the error bars have been omitted when  $\delta(\Delta^{(3)}) < 10$  keV. The open symbols present the experimental values around the shell-gap prior to this work. The data points for  $N = 82$  are beyond the scale.

neutrons and protons) was adjusted so as to give the average pairing gap in  $^{120}\text{Sn}$  equal to 1.245 MeV. The pairing channel was described within the Hartree-Fock-Bogoliubov (HFB) approximation and the blocking and filling approximations [27,28] were used to treat odd nuclei.

First, to provide a baseline for further analyses, in Fig. 4 we show the neutron  $\Delta^{(3)}$  staggering calculated within the spherical approximation [29]. Such an approximation allows us to look at pure effects of pairing correlations, whereby the binding energies of odd isotopes are decreased due to one pair being broken. Otherwise, in this approximation, effects due to deformation polarizations exerted by valence particles are completely switched off. From Fig. 4(b) we see that for the volume (vol) or mixed (mix) pairing forces [30], the experimental decrease of  $\Delta^{(3)}$  when crossing the  $N = 82$  gap in Sn is very well reproduced, whereas the data exclude the pure surface pairing force. Such pairing decrease is due to a lower level density above

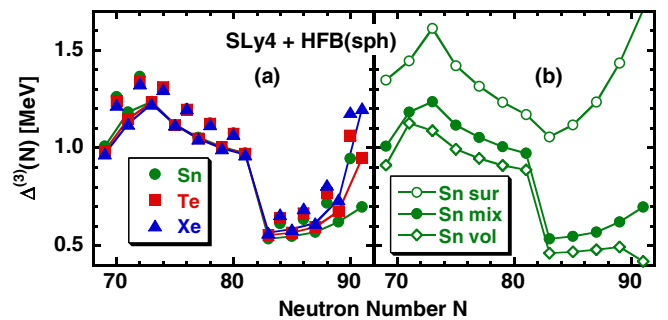


FIG. 4 (color online). The same as in Fig. 3 but for the calculated (spherical HFB) odd-even mass staggering in (a) Sn, Te, and Xe isotope chains and mixed pairing force and (b) Sn isotope chain and surface, mixed, and volume pairing forces.

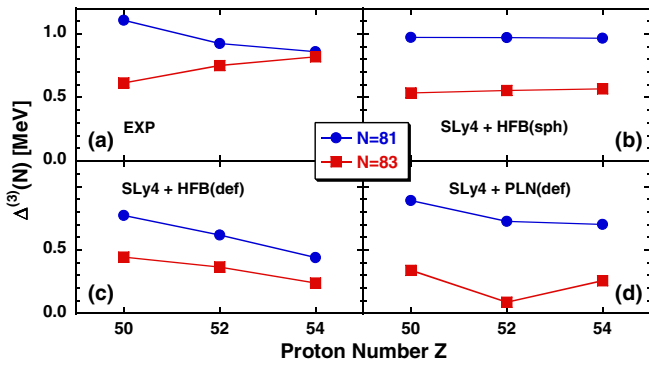


FIG. 5 (color online). Odd-even staggering for the  $N = 81$  and  $83$  isotones as measured in experiment (a) and estimated within the spherical (b), deformed (c), and deformed particle-number-conserving (d) self-consistent calculations.

the  $N = 82$  gap [4] (the surface pairing force is unable to discriminate between the two surface-type orbitals  $\nu h_{11/2}$  and  $\nu f_{7/2}$  located below and above the  $N = 82$  shell gap, respectively). Spherical calculations miss the experimental values in Te and Xe isotopes [Fig. 4(a)], which indicates that the polarization effects must here be taken into account explicitly.

To better illustrate the trends in  $Z > 50$  nuclei, in Fig. 5 we show the experimental neutron  $\Delta^{(3)}$  staggering in Sn, Te, and Xe isotopes along the  $N = 81$  and  $83$  lines, compared with theoretical results. In experiment [Fig. 5(a)], the difference between the  $N = 81$  and  $83$  isotones smoothly decreases from about 0.5 MeV in Sn to almost zero in Xe, whereas spherical results [discussed above and repeated in Fig. 5(b)] show no such decrease at all.

To analyze the effects of polarizations induced by deformation, we have performed two additional HFB calculations. First, by using the code HFODD (v2.51i) [31], we allowed valence particles or holes to induce self-consistently deformed shapes. Then, the even isotones,  $N = 80, 82,$  and  $84,$  turn out to be spherical anyhow; namely, neither do the closed-core  $N = 82$  systems become deformed, nor do the paired two neutron particles or holes induce nonzero deformations. Only the polarization effects exerted by unpaired odd neutron particles or holes are strong enough to induce nonzero deformations in the odd isotones,  $N = 81$  and  $83.$

In this way, the odd-particle polarizations lead to lower values of the  $\Delta^{(3)}$  staggering solely through increased binding energies of odd isotones. Since such polarization increases with adding protons, the obtained values of  $\Delta^{(3)}$  decrease with  $Z,$  as illustrated in Fig. 5(c). However, this trend does not depend on whether deformation is induced by odd particles or holes; therefore, on both sides of the  $N = 82$  shell gap we obtain an identical decrease with  $Z,$  at variance with experiment.

To test if the above results may be affected by the particle-number nonconservation inherent in the HFB the-

ory, we have repeated all calculations by using the HFBTHO code [32,33]. Here, within the Lipkin-Nogami method, we were able to include the approximate particle-number projection after variation. Moreover, the obtained solutions were next exactly projected on good particle numbers. Such a projected Lipkin-Nogami method was extensively tested [33] and proved to be very efficient in describing pairing correlations in near-closed-shell systems.

The obtained results are shown in Fig. 5(d). We see that the general pattern is not qualitatively changed. The dynamic pairing correlations, which are now nonzero even in the  $N = 82$  isotones, lead to larger values of the  $\Delta^{(3)}$  staggering, which in the  $N = 81$  isotones perfectly well reproduce the experimental trend. However, in the  $N = 83$  isotones, the disagreement with data remains a puzzle. Indeed, the asymmetry of the trend of the staggering, measured below and above the  $N = 82$  gap, points to specific effects related to orbitals occupied beyond  $N = 82$  or to their weak binding, which are not captured by the current state-of-the-art theoretical approaches.

This work has been supported by the Academy of Finland under the Centre of Excellence Program 2006–2014 (Nuclear and Accelerator Based Physics Program at JYFL) and the FIDIPRO program.

*Note added in proof.*—Recently, another Penning trap study [34] appeared where some isotope masses overlapping with our data set were measured showing excellent agreement.

\*jani.hakala@phys.jyu.fi

†Present address: Max-Planck-Institut für Kernphysik, Saupfercheckweg 1, 69117 Heidelberg, Germany.

‡juha.aysto@phys.jyu.fi

- [1] P. Hoff *et al.* (ISOLDE Collaboration), *Phys. Rev. Lett.* **77**, 1020 (1996).
- [2] K. L. Jones *et al.*, *Nature (London)* **465**, 454 (2010).
- [3] D. C. Radford *et al.*, *Phys. Rev. Lett.* **88**, 222501 (2002).
- [4] J. Terasaki, J. Engel, W. Nazarewicz, and M. Stoitsov, *Phys. Rev. C* **66**, 054313 (2002).
- [5] M. P. Kartamyshev, T. Engeland, M. Hjorth-Jensen, and E. Osnes, *Phys. Rev. C* **76**, 024313 (2007).
- [6] W. Satuła, J. Dobaczewski, and W. Nazarewicz, *Phys. Rev. Lett.* **81**, 3599 (1998).
- [7] K. Blaum, *Phys. Rep.* **425**, 1 (2006).
- [8] M. Dworschak *et al.*, *Phys. Rev. Lett.* **100**, 072501 (2008).
- [9] D. Neidherr *et al.*, *Phys. Rev. C* **80**, 044323 (2009).
- [10] M. Arnould, S. Goriely, and K. Takahashi, *Phys. Rep.* **450**, 97 (2007).
- [11] A. Jokinen, T. Eronen, U. Hager, I. Moore, H. Penttilä, S. Rinta-Antila, and J. Äystö, *Int. J. Mass Spectrom.* **251**, 204 (2006).
- [12] H. Penttilä *et al.*, *Eur. Phys. J. A* **25**, 745 (2005).
- [13] G. Savard, St. Becker, G. Bollen, H.-J. Kluge, R. B. Moore, Th. Otto, L. Schweikhard, H. Stolzenberg, and U. Wiess, *Phys. Lett. A* **158**, 247 (1991).

- [14] T. Eronen, V.-V. Elomaa, U. Hager, J. Hakala, A. Jokinen, A. Kankainen, S. Rahaman, J. Rissanen, C. Weber, and J. Äystö, *Nucl. Instrum. Methods Phys. Res., Sect. B* **266**, 4527 (2008).
- [15] M. König, G. Bollen, H.-J. Kluge, T. Otto, and J. Szerypo, *Int. J. Mass Spectrom. Ion Process.* **142**, 95 (1995).
- [16] S. George, K. Blaum, F. Herfurth, A. Herlert, M. Kretzschmar, S. Nagy, S. Schwarz, L. Schweikhard, and C. Yazidjian, *Int. J. Mass Spectrom.* **264**, 110 (2007).
- [17] T. Eronen *et al.*, *Eur. Phys. J. A* **48**, 46 (2012).
- [18] J. Hakala *et al.*, *Eur. Phys. J. A* **47**, 1 (2011).
- [19] T. Eronen *et al.*, *Phys. Rev. Lett.* **103**, 252501 (2009).
- [20] G. Audi, A. H. Wapstra, and C. Thibault, *Nucl. Phys.* **A729**, 337 (2003).
- [21] M. Redshaw, B. J. Mount, E. G. Myers, and F. T. Avignone, *Phys. Rev. Lett.* **102**, 212502 (2009).
- [22] M. Redshaw, B. J. Mount, and E. G. Myers, *Phys. Rev. A* **79**, 012506 (2009).
- [23] G. Sikler *et al.*, *Nucl. Phys.* **A763**, 45 (2005).
- [24] M. Breitenfeldt *et al.*, *Phys. Rev. C* **81**, 034313 (2010).
- [25] B. Sun *et al.*, *Nucl. Phys.* **A812**, 1 (2008).
- [26] E. Chabanat, P. Bonche, P. Haensel, J. Meyer, and R. Schaeffer, *Nucl. Phys.* **A635**, 231 (1998).
- [27] G. Bertsch, J. Dobaczewski, W. Nazarewicz, and J. Pei, *Phys. Rev. A* **79**, 043602 (2009).
- [28] N. Schunck, J. Dobaczewski, J. McDonnell, J. Moré, W. Nazarewicz, J. Sarich, and M. V. Stoitsov, *Phys. Rev. C* **81**, 024316 (2010).
- [29] J. Dobaczewski, H. Flocard, and J. Treiner, *Nucl. Phys.* **A422**, 103 (1984).
- [30] J. Dobaczewski, W. Nazarewicz, and M. Stoitsov, *Eur. Phys. J. A* **15**, 21 (2002).
- [31] N. Schunck, J. Dobaczewski, J. McDonnell, W. Satuła, J. A. Sheikh, A. Staszczak, M. Stoitsov, and P. Toivanen, *Comput. Phys. Commun.* **183**, 166 (2012).
- [32] M. Stoitsov, J. Dobaczewski, W. Nazarewicz, and P. Ring, *Comput. Phys. Commun.* **167**, 43 (2005).
- [33] M. V. Stoitsov, J. Dobaczewski, R. Kirchner, W. Nazarewicz, and J. Terasaki, *Phys. Rev. C* **76**, 014308 (2007).
- [34] J. Van Schelt *et al.*, *Phys. Rev. C* **85**, 045805 (2012).